An OSRC-Preconditioned Combined-Field Integral Equation For High-Frequency Electromagnetic Scattering

Van Chien Le, Simon Verbruggen, Paul Escapil-Inchauspé, Carlos Jerez-Hanckes, and Kristof Cools

Abstract – This paper presents a combined-field integral equation (CFIE) for high-frequency electromagnetic scattering by perfectly electrically conducting bodies. The formulation employs a preconditioner based on the approximation of the local magnetic-to-electric operator. Numerical experiments on a unit sphere and the National Aeronautics and Space Administration almond benchmark show that the proposed method reduces solving time by more than 70% compared with the classical CFIE while incurring negligible additional assembly costs.

1. Introduction

The numerical computation of electromagnetic fields scattered by perfect electric conductors (PECs) plays a central role in the analysis of electromagnetic systems. Among the many available techniques, boundary integral equation methods have become one of the most powerful and widely used approaches. Within the boundary integral equation framework, electromagnetic scattering by PECs is commonly formulated using the electric field integral equation (EFIE) and the magnetic field integral equation (MFIE):

$$T_\kappa \boldsymbol{j} = \eta^{-1} \boldsymbol{e}^{inc} \times \mathbf{n}, \tag{1}$$

$$\left(K_\kappa - \frac{1}{2} I\right) \boldsymbol{j} = \boldsymbol{h}^{inc} \times \mathbf{n}, \tag{2}$$

where $\boldsymbol{j}$ denotes the surface electric current density on the boundary Γ, $\mathbf{n}$ is the outward normal vector on Γ, and η is the impedance coefficient of the background medium. The incident electric and magnetic fields $\boldsymbol{e}^{inc}$ and $\boldsymbol{h}^{inc}$ are assumed to originate in the background region and to satisfy Maxwell's equations. The identity operator is denoted by I, and the boundary integral operators T_κ and K_κ associated with the wavenumber κ are defined by

$$\begin{aligned}(T_\kappa \boldsymbol{m})(\boldsymbol{x}) = &-\iota\kappa \mathbf{n} \times \int_\Gamma \frac{e^{-\iota\kappa|\boldsymbol{x}-\boldsymbol{y}|}}{4\pi|\boldsymbol{x}-\boldsymbol{y}|} \boldsymbol{m}(\boldsymbol{y}) \mathrm{d}s_{\boldsymbol{y}} \\ &+ \frac{1}{\iota\kappa} \mathbf{n} \times \mathbf{grad}_{\boldsymbol{x}} \int_\Gamma \frac{e^{-\iota\kappa|\boldsymbol{x}-\boldsymbol{y}|}}{4\pi|\boldsymbol{m}-\boldsymbol{y}|} \, \mathrm{div}_\Gamma \boldsymbol{m}(\boldsymbol{y}) \mathrm{d}s_{\boldsymbol{y}},\end{aligned} \tag{3}$$

$$(K_\kappa \boldsymbol{m})(\boldsymbol{x}) = \mathbf{n} \times p.v. \int_\Gamma \mathbf{grad}_{\boldsymbol{x}} \frac{e^{-\iota\kappa|\boldsymbol{x}-\boldsymbol{y}|}}{4\pi|\boldsymbol{x}-\boldsymbol{y}|} \times \boldsymbol{m}(\boldsymbol{y}) \mathrm{d}s_{\boldsymbol{y}}. \tag{4}$$

Here, $\iota = \sqrt{-1}$ is the imaginary unit and *p.v.* stands for the Cauchy principal value.

When modeling high-frequency scattering problems, both the EFIE and the MFIE suffer from severe ill-conditioning near resonant wavenumbers corresponding to eigenvalues of the interior Maxwell problems. Such resonant wavenumbers become increasingly dense as the frequency increases, leading to pronounced numerical instability. To mitigate these difficulties, various regularization strategies have been proposed. Among them, combined-field integral equations (CFIEs) have emerged as a predominant and robust approach. The classical CFIE is given by [1]

$$\left(\mathbf{n} \times T_\kappa - K_\kappa + \frac{1}{2} I\right) \boldsymbol{j} = \eta^{-1} \mathbf{n} \times (\boldsymbol{e}^{inc} \times \mathbf{n}) - \boldsymbol{h}^{inc} \times \mathbf{n}. \tag{5}$$

Throughout this paper, the coupling parameter is set to 0.5, as this value is known to yield the lowest condition number for (5) [2]. The standard discretization of (5) using Rao–Wilton–Glisson (RWG) basis functions $\{\boldsymbol{f}_n\}$ reads:

$$\left(\mathbf{T}_\kappa + \mathbf{K}_\kappa - \frac{1}{2}\mathbf{G}\right) \mathbf{j} = \eta^{-1} \mathbf{e}^{inc} + \mathbf{h}^{inc}, \tag{6}$$

where

$$\begin{aligned} &[\mathbf{T}_\kappa]_{mn} = \langle \mathbf{n} \times \boldsymbol{f}_m, T_\kappa \boldsymbol{f}_n \rangle, \\ &[\mathbf{K}_\kappa]_{mn} = \langle \boldsymbol{f}_m, K_\kappa \boldsymbol{f}_n \rangle, \qquad [\mathbf{G}]_{mn} = \langle \boldsymbol{f}_m, \boldsymbol{f}_n \rangle, \\ &[\mathbf{e}^{inc}]_m = \langle \mathbf{n} \times \boldsymbol{f}_m, \boldsymbol{e}^{inc} \times \mathbf{n} \rangle, \quad [\mathbf{h}^{inc}]_m = \langle \boldsymbol{f}_m, \boldsymbol{h}^{inc} \times \mathbf{n} \rangle, \end{aligned}$$

with $\langle \cdot, \cdot \rangle$ being the $L^2(\Gamma)$-pairing. Despite the resonance-free nature of the CFIE, the linear system (6) remains ill-conditioned due to the presence of the EFIE

Manuscript received 31 March 2026. This work was supported by the European Research Council (ERC) under the European Union's Horizon 2020 Research and Innovation Program under Grant 101001847, the Chilean ANID grant Fondecyt Regular 1231112, and the Research Foundation – Flanders (FWO) under file ID K219326N.

Van Chien Le, Simon Verbruggen, and Kristof Cools are with the IDLab, Department of Information Technology, Ghent University – imec, 9000 Ghent, Belgium; e-mails: vanchien.le@ugent.be, simon.verbruggen@ugent.be, kristof.cools@ugent.be. Paul Escapil-Inchauspé is with the Faculty of Engineering and Science, Universidad Adolfo Ibáñez, Santiago, Chile; e-mail: paul.escapil@edu.uai.cl. Carlos Jerez-Hanckes is with the Department of Mathematics, KTH Royal Institute of Technology, Stockholm, Sweden, and with INRIA Chile, Santiago, Chile; e-mail: carlosjh@kth.se.

operator T_κ. This ill-conditioning becomes increasingly severe at high frequencies, where dense meshes are required to accurately resolve the oscillating behavior of the electromagnetic fields. An effective remedy is provided by Calderón preconditioning based on a localized EFIE operator T_{κ_ϵ} with a complex wavenumber κ_ϵ, leading to the following Calderón-preconditioned (CP) CFIE [3]:

$$\left(T_{\kappa_\epsilon}T_\kappa + K_\kappa - \frac{1}{2}I\right)\boldsymbol{j} = \eta^{-1}T_{\kappa_\epsilon}(\boldsymbol{e}^{inc}\times\mathbf{n}) + \boldsymbol{h}^{inc}\times\mathbf{n}. \tag{7}$$

The discretization of (7) typically employs the RWG basis functions and their dual, namely the Buffa–Christiansen functions $\{\boldsymbol{g}_n\}$ that are defined on the barycentric refinement of the computational mesh. In particular, the CP-CFIE (7) is discretized as follows [4]:

$$\left(\mathbb{T}_{\kappa_\epsilon}\widetilde{\mathbf{G}}^{-\mathsf{T}}\mathbf{T}_\kappa - \widetilde{\mathbf{K}}_\kappa + \frac{1}{2}\widetilde{\mathbf{G}}\right)\mathbf{j} = \eta^{-1}\mathbb{T}_{\kappa_\epsilon}\widetilde{\mathbf{G}}^{-\mathsf{T}}\mathbf{e}^{inc} - \widetilde{\mathbf{h}}^{inc}, \tag{8}$$

where

$$[\mathbb{T}_{\kappa_\epsilon}]_{mn} = \langle \mathbf{n}\times\boldsymbol{g}_m, T_{\kappa_\epsilon}\boldsymbol{g}_n\rangle, \quad [\widetilde{\mathbf{K}}_\kappa]_{mn} = \langle \mathbf{n}\times\boldsymbol{g}_m, K_\kappa\boldsymbol{f}_n\rangle,$$
$$[\widetilde{\mathbf{G}}]_{mn} = \langle \mathbf{n}\times\boldsymbol{g}_m, \boldsymbol{f}_n\rangle, \quad [\widetilde{\mathbf{h}}^{inc}]_m = \langle \mathbf{n}\times\boldsymbol{g}_m, \boldsymbol{h}^{inc}\times\mathbf{n}\rangle.$$

The formulation (8) yields matrix systems that remain well-conditioned both at high frequencies and near resonances. A related approach with comparable robustness is the Yukawa–Calderón CFIE, which complements the MFIE contribution in (7) with a localized interior MFIE operator. This formulation was introduced in [5], and its well-posedness on Lipschitz domains, together with rigorous conditioning estimates, was established in [6]. However, the reliance on barycentric refinement in the discretization of these formulations entails a substantial increase in assembly time and memory requirements. A potential remedy is the refinement-free Calderón preconditioner developed for the EFIE in [7]. Nevertheless, it is currently unclear how to extend this approach to CFIE formulations.

In this work, we revisit the idea originally proposed in [8] of incorporating an approximate magnetic-to-electric (MtE) operator Λ_ϵ as a preconditioner for the CFIE, leading to the following formulation:

$$\left(\Lambda_\epsilon T_\kappa - K_\kappa + \frac{1}{2}I\right)\boldsymbol{j} = \eta^{-1}\Lambda_\epsilon(\boldsymbol{e}^{inc}\times\mathbf{n}) - \boldsymbol{h}^{inc}\times\mathbf{n}. \tag{9}$$

The operator Λ_ϵ is derived from the on-surface radiation condition (OSRC) method [9] and can be efficiently approximated through the discrete solution of a few elliptic surface differential equations.

Although OSRC-based CFIEs have been introduced in [8] and related works, explicit discretization strategies and implementation details have not been provided in the literature. The objective of the present work is to develop a concrete and practical discretization of (9), based on the MtE approximations proposed in [9, 10]. The resulting linear systems can be assembled at very low additional cost while preserving the favorable conditioning properties of the CFIE. Numerical experiments demonstrate the effectiveness and superior computational efficiency of the proposed method compared to both the classical and Calderón-preconditioned approaches.

2. OSRC-Preconditioned CFIE

2.1 Formulation

The approximate MtE operator is defined as [8, 9]

$$\begin{aligned}\Lambda_\epsilon &= \mathbf{n}\times\left(I - \frac{1}{\kappa_\epsilon^2}\mathbf{curl}_\Gamma\mathrm{curl}_\Gamma\right)^{-1}\left(I + \frac{1}{\kappa_\epsilon^2}\Delta_\Gamma\right)^{1/2} \\ &=: \mathbf{n}\times\Lambda_{1,\epsilon}^{-1}\Lambda_{2,\epsilon},\end{aligned} \tag{10}$$

where a regularizing lossy wavenumber κ_ϵ is introduced to avoid spurious resonances. The operator $\Lambda_{1,\epsilon}^{-1}$ can be discretized into the following:

$$\Lambda_{1,h}^{-1} = (\mathbf{G} - \mathbf{N}_\epsilon)^{-1}, \tag{11}$$

where

$$[\mathbf{N}_\epsilon]_{mn} = \frac{1}{\kappa_\epsilon^2}\langle \mathrm{curl}_\Gamma(\mathbf{n}\times\boldsymbol{f}_m), \mathrm{curl}_\Gamma(\mathbf{n}\times\boldsymbol{f}_n)\rangle.$$

The sparse matrix $\mathbf{G} - \mathbf{N}_\epsilon$ can be readily inverted using a sparse LU decomposition. The pseudo-differential operator $\Lambda_{2,\epsilon}$ can be efficiently evaluated using a rotating branch-cut Padé approximation of order N_p as follows:

$$\Lambda_{2,h} = R_0\left(\mathbf{I} - \frac{1}{R_0}\mathbf{G}\sum_{i=1}^{N_p}\frac{A_i}{B_i}\Pi_{i,\epsilon,h}^{-1}\right), \tag{12}$$

where $\mathbf{I}$ is the identity matrix, and R_0, A_i, B_i $(i = 1, 2, \ldots, N_p)$ are the complex coefficients of the Padé approximation, as specified in [9]. The term $\Pi_{i,\epsilon,h}$ is given by

$$\Pi_{i,\epsilon,h} = \mathbf{G} - B_i(\mathbf{N}_\epsilon + \mathbf{L}\mathbf{M}_\epsilon^{-1}\mathbf{L}^{\mathsf{T}}), \tag{13}$$

where

$$[\mathbf{L}]_{mn} = \langle \mathbf{grad}_\Gamma\phi_m, \mathbf{n}\times\boldsymbol{f}_n\rangle, \quad [\mathbf{M}_\epsilon]_{mn} = \langle \kappa_\epsilon^2\phi_m, \phi_n\rangle,$$

with $\{\phi_n\}$ the set of scalar-valued, continuous, first-order Lagrangian basis functions defined on the surface mesh of Γ. The inversion of $\Pi_{i,\epsilon,h}$ can be efficiently performed via a sparse LU decomposition of the associated mixed-matrix system, as described in [10].

Finally, the operator $\mathbf{n}\times$ is discretized into the matrix $-\mathbf{G}$, which can be seen as a mapping from the Nédélec space spanned by $\{\mathbf{n}\times \boldsymbol{f}_n\}$ into the dual of the RWG space spanned by $\{\boldsymbol{f}_n\}$. The discretization of the approximate MtE operator Λ_ϵ then reads as follows:

$$\Lambda_h = -\mathbf{G}\Lambda_{1,h}^{-1}\Lambda_{2,h}. \tag{14}$$

This matrix maps from the dual Nédélec space into the dual RWG space. Employing a compatible discretization of the MFIE as a mapping from the RWG space to its dual (by testing with the RWG basis functions), we arrive at the following discretization of the OSRC CFIE (9):

$$\left(\Lambda_h\mathbf{T}_\kappa - \mathbf{K}_\kappa + \frac{1}{2}\mathbf{G}\right)\mathbf{j} = \eta^{-1}\Lambda_h\mathbf{e}^{inc} - \mathbf{h}^{inc}. \tag{15}$$

As in the classical CFIE (6), the MFIE component in (15) is discretized nonconformingly. Such nonconforming MFIE discretization is known to be less accurate than the conforming mixed discretization based on Buffa–Christiansen test functions and the EFIE formulation [11–13]. This limitation is also inherited by the OSRC CFIE (15), although the presence of the EFIE contribution mitigates its effect. This observation points to a more fundamental difficulty in the design of CFIEs. Namely, constructing a refinement-free CFIE formulation that is simultaneously resonance-free and conforming in both its EFIE and MFIE components remains challenging.

2.2 Computational Cost

The computation of the OSRC preconditioner Λ_h requires only the solution of a few surface differential equations on Γ, thereby avoiding the assembly of boundary integral operators on barycentric refinements. Numerical results show that, in the moderately high-frequency regime, the evaluation of Λ_h incurs only a negligible additional cost compared with the discretization of the classical CFIE (6), while significantly improving the conditioning of the linear system and, consequently, reducing the overall solution time.

In the very high-frequency regime, where the mesh size is required to decrease at least as fast as the wavelength and the number of degrees of freedom N rapidly increases as a consequence, fast compression techniques may reduce the assembly cost of boundary integral operators on both primal and refined meshes to quasi-linear complexity. In this case, the construction and application of the OSRC preconditioner Λ_h may eventually become the dominant cost because it relies on sparse LU factorizations of finite element matrices, whose complexity scales as $\mathcal{O}(N^{3/2})$ [14]. Nevertheless, the relatively large constants involved in the practical performance of acceleration techniques may postpone the onset of this asymptotic regime until extremely dense meshes are reached. For the mesh sizes typically encountered in practice, the proposed method remains computationally efficient.

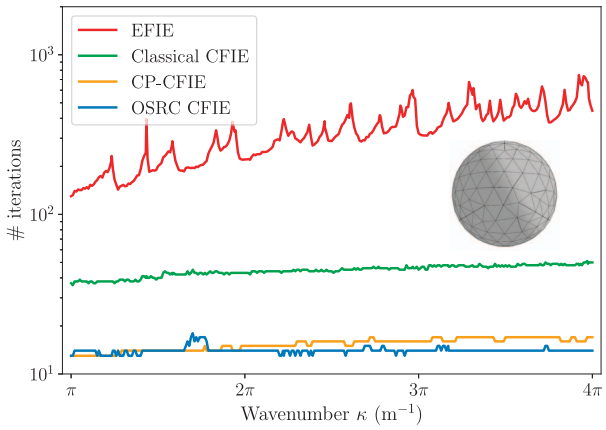


Figure 1. Number of GMRES iterations required to reach a relative tolerance of 10^{-6} as a function of the wavenumber κ for scattering by the unit sphere.

3. Numerical Results

In this section, we present some numerical experiments to validate the effectiveness and computational efficiency of the proposed formulation (15). The background medium is assumed to be free space, and the incident fields are plane waves of the following form:

$$\boldsymbol{e}^{inc}(\boldsymbol{x}) = \hat{\boldsymbol{x}}\exp(-\iota\kappa\hat{\boldsymbol{z}}\cdot\boldsymbol{x}), \tag{16}$$

$$\boldsymbol{h}^{inc}(\boldsymbol{x}) = -\frac{1}{\iota\kappa\eta}\mathbf{curl}\boldsymbol{e}^{inc}(\boldsymbol{x}), \tag{17}$$

where $\hat{\boldsymbol{x}}$ and $\hat{\boldsymbol{z}}$ are the unit vectors along the x- and z-axes, respectively. The regularizing wavenumber is chosen as $\kappa_\epsilon = \kappa - 0.39\iota\kappa^{1/3}$, which was established in [8, 15] as the optimal choice. The average mesh size is set to $h = 0.2\pi/\kappa$ (or equivalently $h = 0.1\lambda$, with λ the wavelength). The Padé approximation is truncated to $N_p = 1$ term. No acceleration technique is employed.

3.1 Scattering by Sphere

We first consider scattering by a unit PEC sphere. Figure 1 presents the number of generalized minimal residual method (GMRES) iterations required to reach a relative tolerance of 10^{-6} for different formulations. As the wavenumber κ increases, or when κ approaches an interior resonance, the EFIE formulation (1) exhibits a rapidly increasing iteration count. Moreover, the density of resonant wavenumbers increases at higher frequencies, further degrading convergence. The classical CFIE (6) is free from resonant instabilities, but its iteration count still grows with κ, although more mildly than that of the EFIE. In contrast, both the CP-CFIE (8) and the

Table 1. Assembly and solving times (in seconds) of different formulations on the unit sphere

	CFIE	CP-CFIE	OSRC CFIE
Assembly			
$\kappa = 2\pi$	31.93	751.10	32.41
$\kappa = 4\pi$	444.09	11678.30	448.61
$\kappa = 6\pi$	2473.88	–	2480.19
$\kappa = 8\pi$	7583.85	–	7596.24
Solving			
$\kappa = 2\pi$	2.03	1.13	0.72
$\kappa = 4\pi$	36.67	19.58	10.56
$\kappa = 6\pi$	217.78	–	58.65
$\kappa = 8\pi$	769.10	–	220.73

Table 2. Assembly and solving times (in seconds) of different formulations on the NASA almond

	CFIE	CP-CFIE	OSRC CFIE
Assembly			
$\kappa = \pi$	44.03	1096.03	44.59
$\kappa = 2\pi$	637.40	16338.12	642.61
$\kappa = 3\pi$	3535.35	–	3542.17
$\kappa = 4\pi$	13865.73	–	13877.63
Solving			
$\kappa = \pi$	4.27	3.37	1.50
$\kappa = 2\pi$	72.14	51.50	22.07
$\kappa = 3\pi$	438.50	–	126.86
$\kappa = 4\pi$	1093.27	–	256.35

OSRC-preconditioned CFIE (15) maintain a nearly constant number of iterations over the entire frequency range considered. Of note, at high frequencies, the OSRC CFIE typically requires fewer iterations than the CP-CFIE.

Next, we examine the computational efficiency of the proposed formulation. Table 1 reports the assembly and solving times of the classical CFIE (6), the CP-CFIE (8), and the OSRC CFIE (15) for different values of the wavenumber κ. The results show that assembling the OSRC preconditioner incurs only a marginal additional cost, while leading to a substantial reduction in solving time. In contrast, the CP-CFIE entails a significant assembly cost due to the discretization and testing of boundary integral operators on barycentrically refined meshes. As a consequence, the assembly and solving times for the CP-CFIE at $\kappa = 6\pi$ and $\kappa = 8\pi$ are prohibitively large and are therefore omitted from Table 1.

3.2 Scattering by the National Aeronautics and Space Administration Almond

In the second experiment, we investigate the performance of the proposed formulation on a more complex surface, namely the National Aeronautics and Space Administration (NASA) almond benchmark. Figure 2 reports the GMRES iteration counts for the different formulations, confirming the effectiveness of the OSRC CFIE in remedying both resonant and dense-mesh ill-conditioning. Table 2 further compares the assembly and solving times of the three CFIE formulations at four wavenumbers ranging from $\kappa = \pi$ to $\kappa = 4\pi$. Owing to the large electrical size of the NASA almond, these values already correspond to the high-frequency regime. Similar to the sphere case, the OSRC CFIE is assembled with a negligible extra cost ($<1\%$) compared with the classical CFIE, while reducing the solving time by more than 70%. These results further demonstrate the superior computational efficiency of the proposed OSRC CFIE formulation over both the classical CFIE and CP-CFIE.

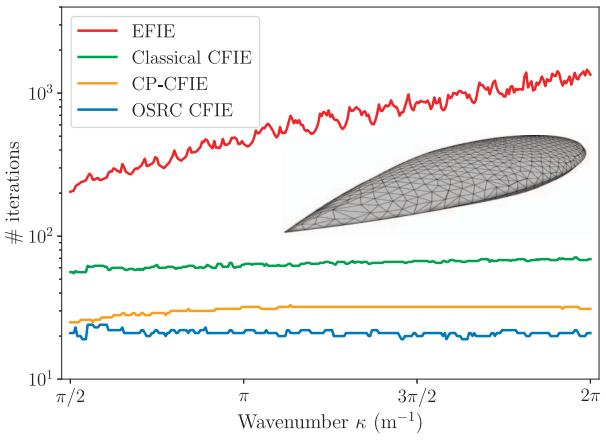


Figure 2. Number of GMRES iterations required to reach a relative tolerance of 10^{-6} as a function of the wavenumber κ for scattering by the benchmark NASA almond of size $9.936 \times 1.92 \times 0.64$ m.

4. Conclusions

We have proposed a CFIE formulation for high-frequency electromagnetic scattering by PECs. The formulation incorporates a preconditioner based on an efficient approximation of a local magnetic-to-electric operator. Numerical results on a PEC sphere and the NASA almond demonstrate that the proposed method effectively suppresses resonant instability and dense-mesh breakdown while maintaining high computational efficiency.

We emphasize that the proposed formulation can be applied straightforwardly to more complex geometries, while retaining the advantage of a negligible assembly cost. Nevertheless, its conditioning properties on such geometries require further investigation, as the resulting preconditioning effect may be less robust than that of Calderón preconditioners. This possible loss of effectiveness can be attributed to the approximation of the MtE operator on non-smooth surfaces and to the use of a truncated Padé approximation of the underlying pseudo-differential operator. Alternative formulations based on local approximations or surrogates to boundary integral operators that avoid the explicit square-root operator in the MtE map, for instance by squaring it as in [16], therefore represent a promising direction for future research.

5. References

1. J. R. Mautz and R. F. Harrington, "H-Field, E-Field, and Combined Field Solution for Conducting Bodies of Revolution," *Archiv für Elektronik und Übertragungstechnik*, **32**, 4, April 1978, pp. 157-164.
2. R. Kress, "Minimizing the Condition Number of Boundary Integral Operators in Acoustic and Electromagnetic Scattering," *The Quarterly Journal of Mechanics and Applied Mathematics*, **38**, 2, May 1985, pp. 323-341.
3. H. Bagci, F. P. Andriulli, K. Cools, F. Olyslager, and E. Michielssen, "A Calderón Multiplicative Preconditioner for the Combined Field Integral Equation," *IEEE Transactions on Antennas and Propagation*, **57**, 10, October 2009, pp. 3387-3392.
4. F. P. Andriulli, K. Cools, I. Bogaert, H. Bagci, P. Yla-Ojiala, and E. Michielssen, "Analysis and Discretization of the Yukawa-Calderon Preconditioned CFIE," 28th Annual Review of Progress in Applied Computational Electromagnetics (ACES - 2012), Columbus, OH, USA, April 10–14, 2012, pp. 454-463.
5. F. P. Andriulli, I. Bogaert, K. Cools, and E. Michielssen, "A Well-Conditioned Combined Field Integral Equation Based on Quasi-Helmholtz Projectors," International Conference on Electromagnetics in Advanced Applications, Torino, Italy, September 9–13, 2013, pp. 644-647.
6. V. C. Le and K. Cools, "An Operator Preconditioned Combined Field Integral Equation for Electromagnetic Scattering," *SIAM Journal on Numerical Analysis*, **62**, 6, 2024, pp. 2484-2505.
7. S. B. Adrian, F. P. Andriulli, and T. F. Eibert, "On a Refinement-Free Calderón Multiplicative Preconditioner for the Electric Field Integral Equation," *Journal of Computational Physics*, **376**, January 2019, pp. 1232-1252.
8. M. Darbas, "Generalized Combined Field Integral Equations for the Iterative Solution of the Three-Dimensional Maxwell Equations," *Applied Mathematics Letters*, **19**, 8, August 2006, pp. 834-839.
9. M. El Bouajaji, X. Antoine, and C. Geuzaine, "Approximate Local Magnetic-to-Electric Surface Operators for Time-Harmonic Maxwell's Equations," *Journal of Computational Physics*, **279**, December 2014, pp. 241-260.
10. I. Fierro-Piccardo and T. Betcke, "An OSRC Preconditioner for the EFIE," *IEEE Transactions on Antennas and Propagation*, **71**, 4, April 2023, pp. 3408-3417.
11. P. Ylä-Oijala, M. Taskinen, and S. Järvenpää, "Surface Integral Equation Formulations for Solving Electromagnetic Scattering Problems With Iterative Methods," *Radio Science*, **40**, 6, December 2005, doi: 10.1029/2004RS003169.
12. K. Cools, F. P. Andriulli, D. De Zutter, and E. Michielssen, "Accurate and Conforming Mixed Discretization of the MFIE," *IEEE Antennas and Wireless Propagation Letters*, **10**, 2011, pp. 528-531.
13. S. Yan, J.-M. Jin, and Z. Nie, "Accuracy Improvement of the Second-Kind Integral Equations for Generally Shaped Objects," *IEEE Transactions on Antennas and Propagation*, **61**, 2, February 2013, pp. 788-797.
14. A. George and E. Ng, "On the Complexity of Sparse *QR* and *LU* Factorization of Finite-Element Matrices," *SIAM Journal on Scientific and Statistical Computing*, **9**, 5, 1988, pp. 849-861.
15. Y. Boubendir and C. Turc, "Well-Conditioned Boundary Integral Equation Formulations for the Solution of High-Frequency Electromagnetic Scattering Problems," *Computers & Mathematics with Applications*, **67**, 10, June 2014, pp. 1772-1805.
16. C. Henry, A. Merlini, and F. P. Andriulli, "Laplacian Surrogate of the EFIE based on Differential Forms: Application to Preconditioning," 25th International Symposium on Electromagnetic Theory (EMTS 2025), Bologna, Italy, June 23–27, 2025.